Design study of low-energy beam transport for multi-charge beams at RAON

Jungbae Bahng, Eun-San Kim
Department of Physics, Kyungpook National University, Sangyok-dong, Daegu, 702-701 Korea
Bong Hyuk Choi
Rare Isotope Science Project, Institute for Basic Science, Daejeon 305-811, Korea
Ji Qiang
Lawrence Berkeley National Laboratory, Berkeley, CA 94720, USA

***Abstract*—The Rare isotope Accelerator Of Newness (RAON) at the Rare Isotope Science Project (RISP) is being designed to simultaneously accelerate beams with multiple charge states. It includes a driver superconducting (SC) linac for producing 400 kW continuous wave (CW) heavy ion beams from protons to uranium. The RAON consists of a few electron cyclotron resonance (ECR) ion sources, a low-energy beam transport (LEBT) system, a CW 81.25 MHz radio frequency quadrupole (RFQ) accelerator, a medium-energy beam transport system, the SC linac, and a charge-stripper system. The LEBT system for the RISP accelerator facility consists of a high-voltage platform, two 90° dipoles, a multi-harmonic buncher (MHB), solenoids, electrostatic quadrupoles, a velocity equalizer, and a diagnostic system. The ECR ion sources are located on a high-voltage platform to reach an initial beam energy of 10 keV/u. After extraction, the ion beam is transported through the LEBT system to the RFQ accelerator. The generated beam is selected by an achromatic bending system and then bunched by the MHB in the LEBT system. The MHB is used to achieve a small longitudinal emittance in the RFQ by generating a sawtooth wave with three harmonics. In this paper, we present the results and issues of the beam dynamics of the LEBT system.**

***Index Terms*—: Low-energy beam transport, Heavy ion accelerator, Multi-harmonic buncher**

I. Introduction

The Rare isotope Accelerator Of Newness (RAON) [1] heavy ion accelerator has been designed as a facility for the Rare Isotope Science Project (RISP). It is under construction to support various cutting-edge science fields. The purpose of the RISP is to produce a variety of stable and rare isotope beams for use in various types of basic scientific research and its applications. RAON will produce a 400 kW continuous wave (CW) rare isotope beam using both the In-Flight Fragment (IF) system and the Isotope Separation On-Line (ISOL) system, as shown in Fig. 1. To accomplish the RISP's purpose, the IF system in the RAON consists of superconducting electron cyclotron resonance (ECR) ion sources, a low-energy beam transport (LEBT) system, a CW 81.25 MHz, 500 keV/u radio frequency quadrupole (RFQ) accelerator, a medium-energy beam transport (MEBT) system, a superconducting (SC) linac, and a charge stripper system. The ISOL system uses a proton cyclotron as a driver. The LEBT system for the driver linac consists of a high-voltage platform, two 90° dipoles, a multi-harmonic buncher (MHB), solenoids, electrostatic quadrupoles (ESQs), a velocity equalizer, and a diagnostic system. The ECR ion sources are located on a high-voltage platform to reach an initial beam energy of 10 keV/u. After extraction, the ion beam is transported through the LEBT system to the RFQ accelerator using the ESQs and solenoids. The generated beam is selected by an achromatic bending system and then bunched by the MHB in the LEBT. The MHB is used to achieve a small longitudinal emittance in the RFQ and to increase the bunching efficiency by generating a sawtooth wave with three harmonics. The LEBT system has two main functions: to select the charged beam from a mixed beam generated from an ion source, and to provide transverse and longitudinal matching to the RFQ accelerator. We present the methods of beam transport and bunching of dual beams in detail.

e-mail: eskim1@knu.ac.kr

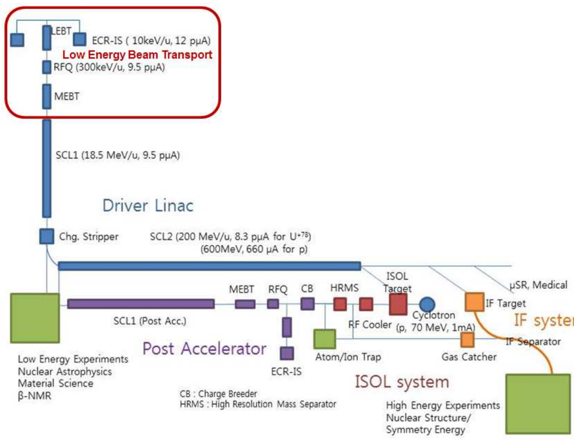

Fig. 1. Layout of the RISP accelerator system

II. LEBT System

A. General remarks

The design goal of a 200 MeV/u, 400 kW uranium beam can be realized by increasing the beam intensity. The simultaneous acceleration and transport of beams with multiple charge states will be attempted to achieve the goal. It is difficult to transport a dual charge state beam because it has a large momentum spread, which causes emittance growth. Therefore, we adopt an achromatic analyzing system to minimize the transverse emittance growth. Additionally, an ESQ lens is used instead of a magnetic quadrupole magnet to focus the beam in the transverse direction because multi-charge beams can be transported using an ESQ. The reason is described in detail in the following section.

B. *ESQ versus quadrupole magnet*

A quadrupole magnet is generally used in an accelerator system to focus an ion beam in the transverse direction; however, an ESQ is very convenient for ion beam focusing, particularly in the low-energy state of beam transport. Ion beam focusing using an ESQ lens to provide an electric force is more efficient than using a quadrupole magnet to provide a magnetic force in the low-energy region. Moreover, using an ESQ makes it possible to transport dual beams because the focusing coefficient of an ESQ does not depend on the charge-to-mass ratio. The focusing coefficient of a magnetic quadrupole (k_M) is given by

$$B \cdot \rho = \frac{1}{q}\sqrt{2 \cdot m \cdot KE}, \tag{1}$$

$$k_M = \frac{qB_0}{\gamma m a \beta c} = \frac{B_0}{a}\frac{q}{qB \cdot \rho} = \frac{B_0}{a}\sqrt{\frac{1}{2U_0}}\sqrt{\frac{q}{m}}, \tag{2}$$

where $B \cdot \rho$ is the magnetic rigidity, q is the charge number of the particles, m is the particle mass, KE is the kinetic energy of the particles, a is the bore radius of the quadrupole magnet, β and γ are relativistic factors, U_0 is the extraction voltage, and B_0 is the magnetic strength of the quadrupole magnet [2].

The focusing coefficient of the ESQ is given by

$$E \cdot \rho = \frac{2 \cdot KE}{q} = \frac{2qU_0}{q} = 2U_0, \tag{3}$$

$$k_E = \frac{qE_0}{\beta^2 c^2 \gamma m a} = \frac{2V_0 q}{a^2 \beta^2 c^2 \gamma m} \tag{4}$$

$$= \frac{2V_0}{a^2}\frac{q}{2KE} = \frac{2V_0}{a^2}\frac{1}{(E \cdot \rho)} = \frac{V_0}{a^2 U_0}, \tag{5}$$

where $E \cdot \rho$ is the electric rigidity, a is the bore radius of the quadrupole lens, and V_0 is the electrode voltage of the ESQ [2]. Thus, the focusing coefficient of the quadrupole magnet (k_M) is proportional to the square root of the mass-to-charge ratio of the particle, whereas the ESQ lens's focusing coefficient k_E depends only on the kinetic energy of the particles, as shown in Eqs. 2 and 5. Dual beams with different charge states are focused with equal strength by the ESQ because, regardless of the charge state of the beam, the focusing coefficient k_E depends only on the extraction voltage, i.e., the particle's kinetic energy.

III. Design Result

A. *Single charge transport*

The MHB has a fundamental RF frequency of 40.625 MHz, and its second and third harmonics are used. The velocity equalizer is operated at 40.625 MHz. Fig. 2 shows the layout of the LEBT system. To realize an achromatic system between dipoles, four triplets are used with mirror symmetry. The desired ion species and charge states will be selected, and the others will be filtered by an analyzing system. After selection, two doublets and a pair solenoid are used to meet the required beam parameters at the entrance of the RFQ; the MHB and velocity equalizer provide bunched beams alternately to the RFQ.

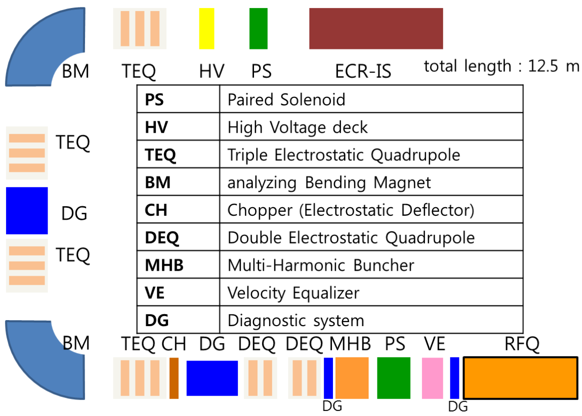

Fig. 2. Layout of the LEBT system

The TRANSPORT [3] code was used to design the second-order achromatic model of the LEBT system from the beam extraction hole of the ECR ion source to the entrance of the RFQ. The lattice of the LEBT system has mirror symmetry about the center of the analyzing section to realize achromaticity. For this simulation, we set an initial momentum deviation of 0.75%, which is based on the energy spread of U^{33+} and U^{34+} beams. A $U^{33.5+}$ beam is used because the TRANSPORT code can calculate the matrices only for particles in a single charge state. Because the beam conditions cannot be measured immediately after beam extraction from the ECR ion sources owing to superposition of various beams, we use the obtained parameters after beam separation. All the ion beams are assumed to have the same Twiss parameters at a hole with a beam waist radius of 5 mm, which is the plasma extraction aperture. A normalized RMS uranium beam emittance of 0.1 πmm mrad is used. Fig. 3 shows the optics designed for the LEBT system for a single charge state $U^{33.5+}$ beam. The length of the designed LEBT system is 12.5 m. We used the RMS size of the beam for the LEBT design in this calculation. The result of the optics design shows that the LEBT system has mirror symmetry in the analyzing section and is achromatic after the analyzing section. The envelope of the half-beam size is less than 1.2 cm and meets the required beam parameters of the RFQ. Because we used 3D field data for a realistic simulation, the results of the TRANS-

PORT, TRACK [4], and IMPACT [5] codes differ in places where TRACK and IMPACT use field maps of elements. We matched the results of TRANSPORT, TRACK, and IMPACT by conducting separate simulations.

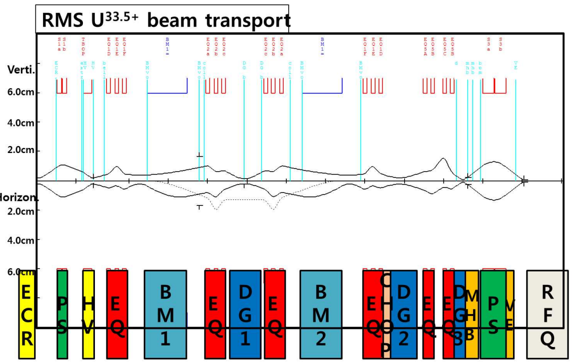

Fig. 3. Designed beam optics for $U^{33.5+}$

The analyzing dipole magnets are designed without edge angles and with a gradient pole field ($n = 0$), radius of curvature $\rho = 0.65$ m, and bending angle $\theta = 90°$. A pair solenoid is used to remove the rotation component caused by focusing in the solenoid [6]. This has an effect to varify the emittance growth in the transverse direction by decoupling the rotation of the beam. Table I shows the elements of the LEBT system. The designed maximum strength of the solenoid is less than 5.0 kG, and the maximum voltage applied in the ESQ lens is less than 35 kV.

Lorem ipsum dolor sit amet, consectetuer adipiscing elit. Ut purus elit, vestibulum ut, placerat ac, adipiscing vitae, felis. Curabitur dictum gravida mauris. Nam arcu libero, nonummy eget, consectetuer id, vulputate a, magna. Donec vehicula augue eu neque. Pellentesque habitant morbi tristique senectus et netus et malesuada fames ac turpis egestas. Mauris ut leo. Cras viverra metus rhoncus sem. Nulla et lectus vestibulum urna fringilla ultrices. Phasellus eu tellus sit amet tortor gravida placerat. Integer sapien est, iaculis in, pretium quis, viverra ac, nunc. Praesent eget sem vel leo ultrices bibendum. Aenean faucibus. Morbi dolor nulla, malesuada eu, pulvinar at, mollis ac, nulla. Curabitur auctor semper nulla. Donec varius orci eget risus. Duis nibh mi, congue eu, accumsan eleifend, sagittis quis, diam. Duis eget orci sit amet orci dignissim rutrum.

B. Dual beam transport

Beam simulations using the TRACK and IMPACT codes are used for 6D tracking that includes the space charge effect. The initial beam distributions shown in Fig. 4 correspond to the initial parameters used for the TRANSPORT code. The normalized RMS emittance in the transverse direction of the uranium beam is assumed to be 0.1 πmm mrad for each charge state of the beam. The emittance values are taken from the measured results of the Versatile ECR Ion Source for Nuclear Science (VENUS) ion source, which was developed at the Lawrence Berkeley National Laboratory [7], with an intrinsic energy spread of 0.05% and CW conditions. The various ion beams extracted from the ECR ion sources are separated by the analyzing system, and the desired ion beam is selected by a collimator. To achieve better separation, the beam is designed to be small at the collimator, and the dispersion function is designed to be as large as possible. Ion beams appeared with good separation at the collimator, as shown in Fig. 5. A chopper and collimator provide the appropriate beam power within the acceptance of the linac by controlling the beam intensity in the LEBT system. The intrinsic DC beam is converted to a bunched beam by the MHB. The MHB requires a small circular beam. Fig. 6 shows the distributions of a dual charge state beam upstream of the MHB. The tracking result of the dual beam shows a 100% transmission rate, reasonable emittance growth in the transverse direction, and a small (within 4 cm) maximum beam envelope, as shown in Fig. 7. The size of the beamline is 6 cm on the basis of the maximum value of the beam envelope. Emittance growth occurs in the solenoid, which rotates the dual beams by different amounts depending on their charge state, so the entire emittance in the transverse direction becomes large compared to that for single beam transport.

IV. Bunching System

The SC linac in the RAON demands a small longitudinal emittance beam, which requires an additional prebunching system upstream of the RFQ. The buncher operates at 40.625 MHz and its second and third harmonics. The three harmonic waves provide a sawtooth wave to achieve high bunching efficiency. The external bunching system enables the design of a shorter RFQ. Bunchers are used to change DC beams into pulsed beams. An oscillating electric field in the buncher affects the energy of charged particles; ideally, the charged particles that arrive at the buncher fast are slowed down, and those arriving last are sped up. The beam passes through the buncher, gaining oscillating energy, and then is focused at a focal point after the drift space. The magnitude of the electric field in the buncher is determined by the focal length. The bunching efficiency is related to the peak-to-peak ratio of the electric field in the buncher. We attempt to increase the peak-to-peak ratio and obtain a small longitudinal emittance by using a sawtooth wave instead of a sine wave.

A. Sawtooth wave

The electric field consists of a geometric component and a time component. The time component causes particle bunching. Using a sine waveform generally yields a bunching efficiency of 50%. To improve the efficiency, we modify the waveform instead of using a sine wave. In Fig. 8, the definition of bunching used in this paper is illustrated using a sine wave. The effective length is the peak-to-peak distance of the sine wave. The ratio of the effective length to the wavelength gives the ratio of the bunched beam to the continuous beam. The derived function $g(x)$ is a linear function that joins the upper and lower peak points.

TABLE I
ELEMENTS OF LEBT SYSTEM

Element	Number	Strength	Unit	Notes
Dipole	2	2.5	kG	$\rho = 0.65$ m $\theta = 90°$ $n = 0$
ES triplet	4	35	kV	eff. length = 3 × 0.10 m
ES doublet	2	35	kV	eff. length = 2 × 0.10 m
Pair solenoid A	1	4.2	kG	eff. length = 2 × 0.13 m
Pair solenoid B	1	5.0	kG	eff. length = 2 × 0.30 m

The aberration is the maximum difference between $f(x)$ and $g(x)$. It is the dominant factor determining the bunch length. To achieve a short bunch length, the aberration must be small.

The waveforms determine the number of harmonics, as shown in Fig. 9. By increasing the number of harmonics, the bunching efficiency is increased and the aberration is decreased. Table II lists the efficiency and aberration for each waveform. The increment of the bunching efficiency and the decrement of the aberration diminish gradually over three harmonics. Although higher harmonics have advantages with respect to the beam quality, it becomes more difficult to manufacture the buncher. A three-harmonic buncher was chosen to realize reasonable beam quality and manufacturability.

A.0.a . Lorem ipsum dolor sit amet, consectetuer adipiscing elit. Ut purus elit, vestibulum ut, placerat ac, adipiscing vitae, felis. Curabitur dictum gravida mauris. Nam arcu libero, nonummy eget, consectetuer id, vulputate a, magna. Donec vehicula augue eu neque. Pellentesque habitant morbi tristique senectus et netus et malesuada fames ac turpis egestas. Mauris ut leo. Cras viverra metus rhoncus sem. Nulla et lectus vestibulum urna fringilla ultrices. Phasellus eu tellus sit amet tortor gravida placerat. Integer sapien est, iaculis in, pretium quis, viverra ac, nunc. Praesent eget sem vel leo ultrices bibendum. Aenean faucibus. Morbi dolor nulla, malesuada eu, pulvinar at, mollis ac, nulla. Curabitur auctor semper nulla. Donec varius orci eget risus. Duis nibh mi, congue eu, accumsan eleifend, sagittis quis, diam. Duis eget orci sit amet orci dignissim rutrum.

B. Design of MHB

The MHB is designed to have two drift tubes that are connected to RF voltages of opposite sign, as shown in Fig. 10. The electrode length and cavity length are designed to minimize the effect of the fringe field. The geometry of the designed MHB is described in Table III. The beam dynamics require an inner diameter of the electrodes of 15 mm and a voltage gap of 4 mm. Both electrodes were designed to be conical to avoid the effect of the fringe field at the outer edge of the electrode [8]. The designed MHB operates at 40.625, 81.25, and 121.625 MHz. The fundamental frequency is determined as half of the RFQ frequencies used alternately to transport multi-charge beams. The electromagnetic field distributions in the MHB from an MWS simulation are shown in Fig. 11. The strength of the electric field at the gap center of the MHB is about 7.5 times that of the fringe field.

TABLE III
GEOMETRY OF THE BUNCHER

Element	Value
Electrode gap	4 mm
Electrode length	25 mm
Inner diameter	15 mm
Electrode angle	30°
Electrode thickness	1 mm

C. Multi-charge beam transport line

The RISP accelerator provides multi-charge beams to increase the beam intensity. Alternating beam bunching is an important issue for achieving multi-charge beam acceleration. After passing through the MHB, dual charge beams are bunched by longitudinal separation because the extraction energy differs according to the charge state. By using separation, dual charge beams can be accelerated by alternating the RF bucket of the RFQ accelerator. To accomplish this goal, the distance L between the MHB and the entrance of the RFQ must satisfy the following equations.

$$\gamma_{1,2} = 1 + \frac{q_{1,2}U}{m}, \tag{6}$$

$$L = \frac{1}{f}\left(\frac{1}{\beta_1 \times c} - \frac{1}{\beta_2 \times c}\right)^{-1}, \tag{7}$$

where U is the extraction voltage, q is the charge number of the particles, m is the particle mass, γ and β are relative coefficients, f is the frequency of the RFQ, and β_1 and β_2 are the velocities of the two beams. For a uranium beam, this yields an acceleration voltage U of 71.04 kV, where $q1$ and $q2$ are 33 and 34, respectively. Thus, the required distance between the MHB and the velocity equalizer is 1.4 m. It is necessary to calculate the field strength of

TABLE II
Bunching efficiency and voltage coefficients

Harmonic	Efficiency	Aberration	U1	U2	U3	U4	U5
First	50.00%	0.210	1	0	0	0	0
Second	63.92%	0.0832	1	0.33	0	0	0
Third	71.48%	0.0481	1	0.38	0.17	0	0
Fourth	75.98%	0.0325	1	0.42	0.20	0.10	0
Fifth	79.20%	0.0246	1	0.44	0.23	0.12	0.07

the MHB. We know the particle energy and the distance between the MHB and the entrance of the RFQ. Thus, we can calculate the flight time,

$$t = \frac{L}{\beta c} = L(\frac{m}{2E_0})^{\frac{1}{2}}, \tag{8}$$

where E_0 is the particle's energy. Eq. 8 is differentiated with respect to E as follows:

$$\frac{dt}{dE} = -\frac{L\sqrt{m}}{2\sqrt{2}}E_0^{-\frac{3}{2}}. \tag{9}$$

Eq. 9 represents how the particle's drift time change with the energy. An oscillating buncher field is represented as V_0cosωt, where ω is the oscillation frequency. Differentiating with respect to time yields

$$\frac{dE}{dt} = q\omega V_0 sin\omega t. \tag{10}$$

The maximum values of Eqs. 11 and 9 yield

$$V_0 = 140.0125\frac{E_0^{\frac{3}{2}}}{fqL\sqrt{m}}, \tag{11}$$

where E, m, and f have units of keV, amu, and MHz, respectively. Evaluating this equation for a $U^{33.5+}$ beam yields a value of 676.029 V.

D. Tracking results

The longitudinal beam distributions for a single charge beam are shown after the MHB and at the entrance of the RFQ in Fig. 12(a) and (b), respectively. Table IV shows that the bunching efficiency is increased from 54% to 75% by using the MHB. In addition, the MHB also minimizes the longitudinal beam emittance. Fig. 13(a)–(e) show the longitudinal beam distributions of a dual charge state beam with alternating bunching before the MHB, after the MHB, before the velocity equalizer, after the velocity equalizer, and at the entrance of the RFQ, respectively. The dual beam is used to increase the beam power to meet a user's requirement. Alternating injection of the dual beam to the linac system can be achieved by using the MHB and velocity equalizer, as illustrated in in Fig. 13(f), which shows the longitudinal distribution at injection into the RFQ. By using the MHB, we achieved a bunching efficiency of 76% in 60° and 65% in 30° for a dual charge beam.

TABLE IV
Comparison of bunching efficiency of single and triple harmonic buncher for single beam

	Single-freq. buncher	Triple-freq. buncher
60°	66.9532%	83.0468%
30°	54.8980%	75.9896%
15°	46.9012%	70.7917%
10°	42.7829%	68.5726%
5°	34.0864%	58.1168%

V. Summary

Beam transport in the RAON and simulation of the LEBT system were presented. We attempted multi-charge beam transport in the LEBT system to increase the beam power. To achieve this goal, the LEBT system is designed with ESQs, a buncher, and a velocity equalizer, which provide an alternating bunched beam and transverse focusing regardless of the charge state of the beam. The LEBT system consists of a high-voltage deck at 47 kV, two 90° dipoles to realize achromaticity, four ESQs, two solenoids, an MHB, a velocity equalizer, and a diagnostic system. Uranium ion beams in multiple charge states have been tracked from the extraction hole of the ECR ion sources to the entrance of the RFQ through the LEBT system while maintaining a 100% transmission rate. The beam emittance growth is small and meets the RAON baseline requirement. An MHB is used instead of a single buncher to increase the bunching efficiency and minimize the longitudinal beam emittance. The bunching efficiency increases from 50% to 75% when the MHB is used, and the aberration of the bunches decreases around one-fifth. The longitudinal emittance at the entrance of the RFQ is 0.3339375 keV/uns for dual beams when the MHB is used. In the LEBT system, we achieved the goals of beam selection, dual beam transport, and meeting the beam parameters at the entrance of the RFQ. After the technical design of all the elements is complete, we plan to conduct more realistic LEBT simulations.

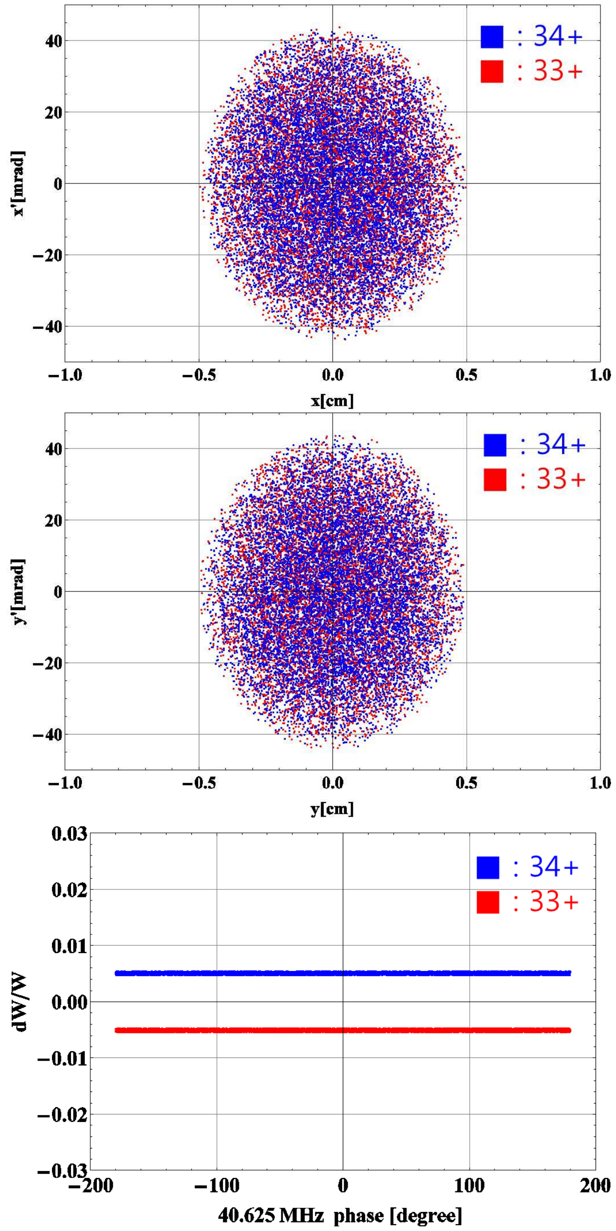

Fig. 4. Initial beam distributions for U^{33+} and U^{34+}

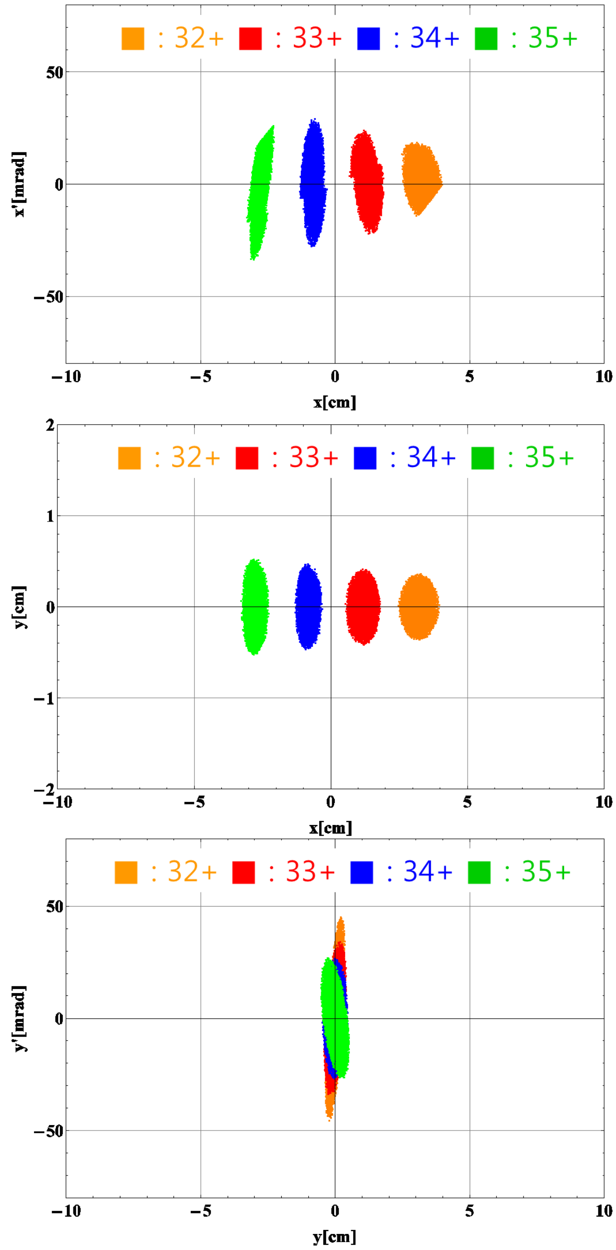

Fig. 5. Beam distributions for selection at slit

VI. Acknowledgments

This work was made possible by the support of the Ministry of Science, ICT and Future Planning (MSIP), the Ministry of Technology, and the National Research Foundation (NRF) of the Republic of Korea under Contract 2011-0032011.

References

[1] D. Jeon, et al., Proceedings of IPAC2013, Sanhai, China, TH-PWO062, 2013.

[2] Martin Resier, *TheoryandDesignofchargedparticlebeams*, Second edition 2008.

[3] K.L. Brown et al. PSI Graphic Transport Framework by U. Rohrer Based on a CERN-SLACFERMILAB Version.

[4] P.N. Ostroumov, K.W. Shepard, Physical Review Special TopicsAccelerators and Beams 11 (2001) 030101.

[5] J. Qiang, R. Ryne, S. Habib, and V. Decyk, J. of Comp. Phys., vol 163, p. 434 (2000).

[6] J. Bahng, et, al., Nuclear Instruments And Method A 769, 9-15 (2015).

[7] J.Gallardo et. al., Proceedings of The 1999 Particle Accelerator Conference, New Yok, USA, 1999, p.3032

[8] J. Sario, J. Gustafsson, P. Kotilainen, K. Kaski, A. Lassila, E. Liukkonen, Beam buncher for the K130-cyclotron, Nuclear Instruments and Method A 370 (1996).

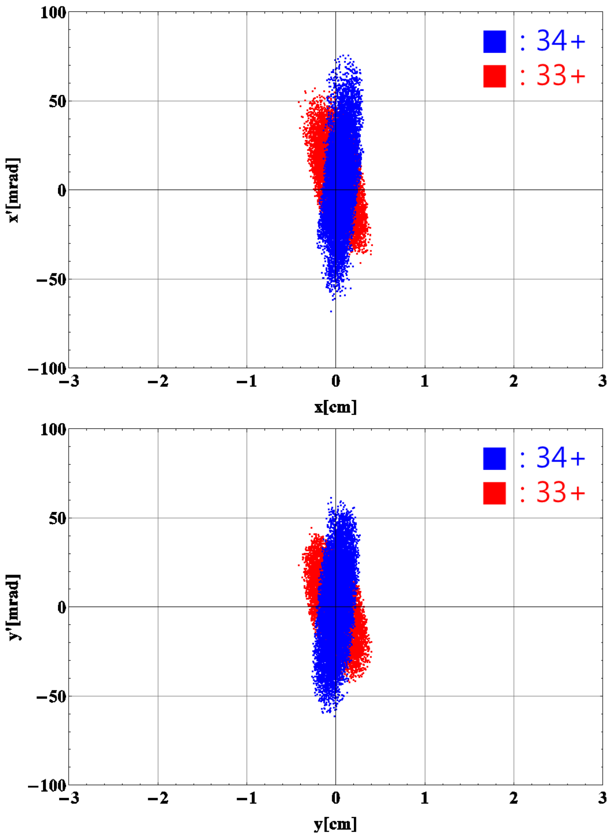

Fig. 6. Beam distributions upstream of MHB

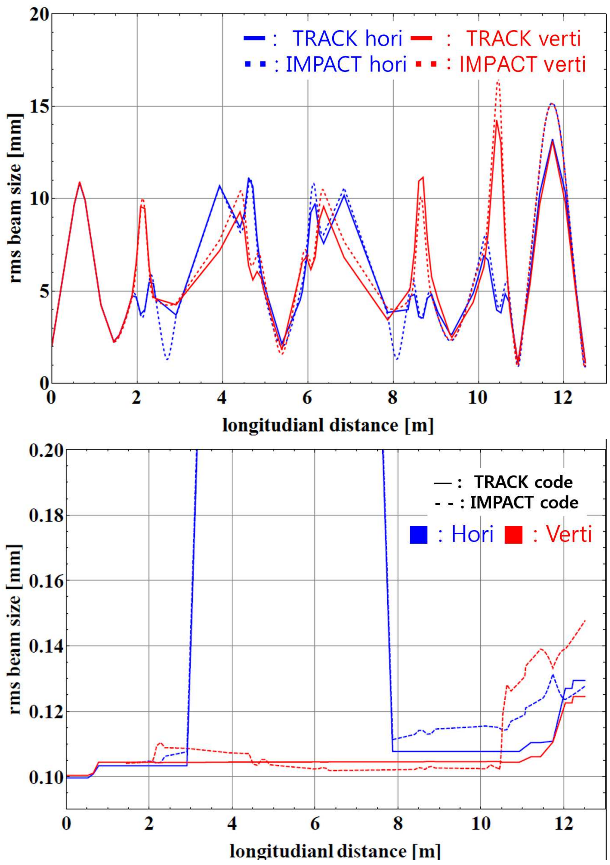

Fig. 7. Result of beam tracking simulation for dual charge state beam

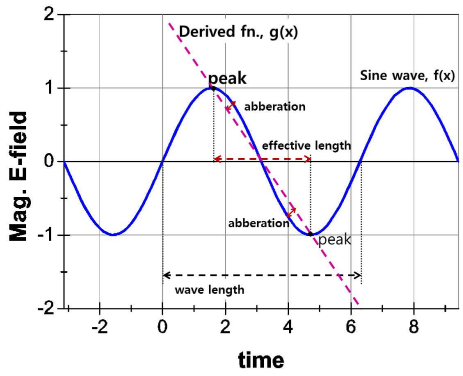

Fig. 8. Definition of bunching

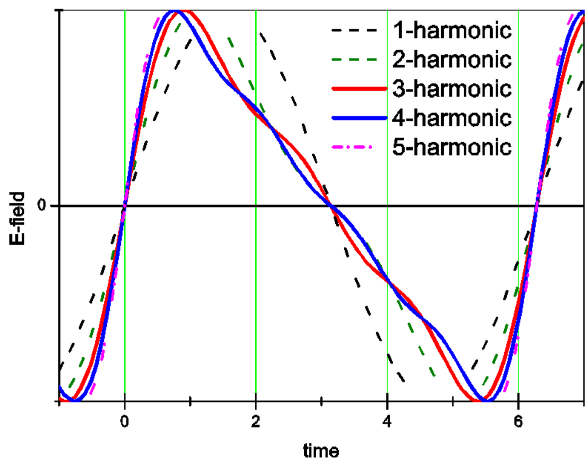

Fig. 9. Waveforms of different harmonics

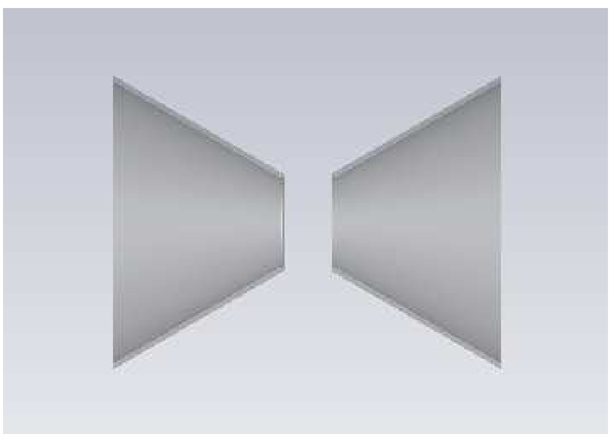

Fig. 10. Structure of the buncher

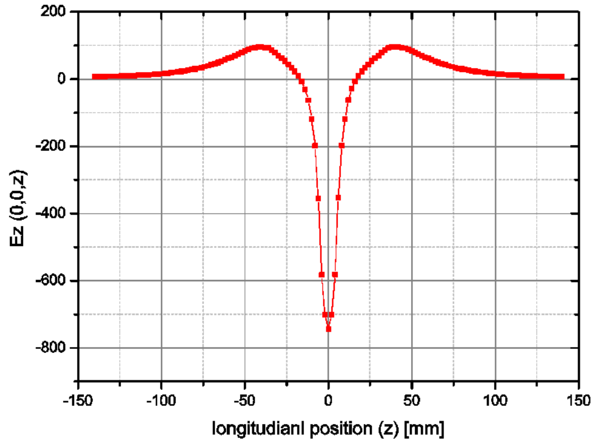

Fig. 11.   2D electric field distributions in MHB

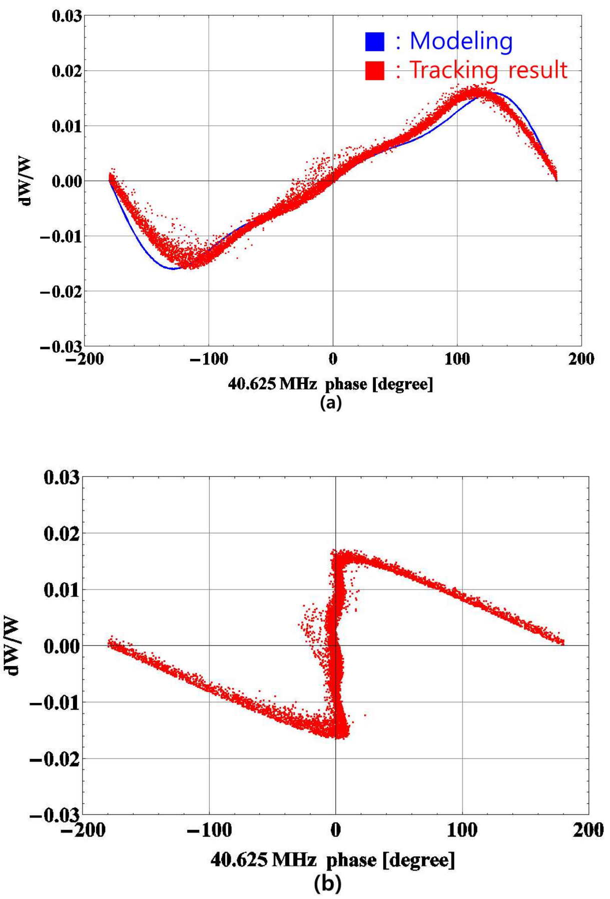

Fig. 12.   Longitudinal beam distributions for single charge state beam (a) Downstream of the MHB (b) At entrance of the RFQ

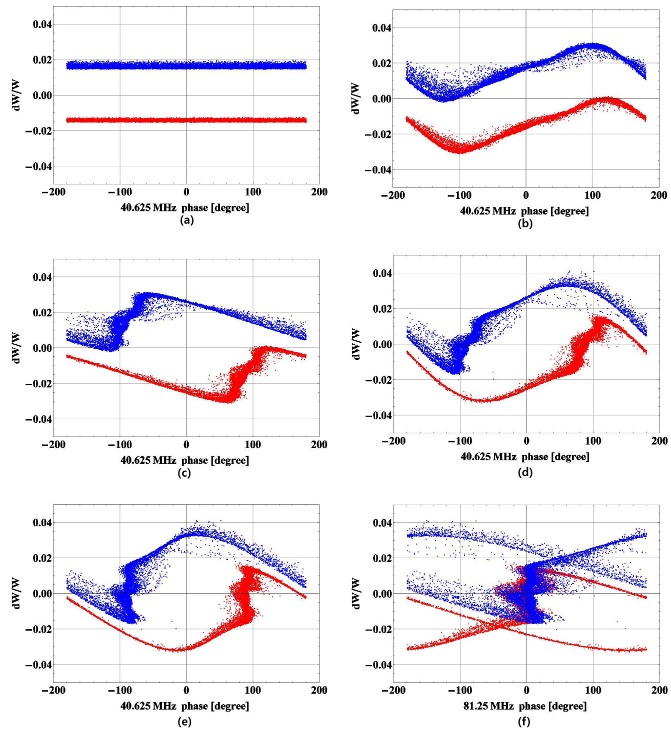

Fig. 13.   Longitudinal beam distributions for alternating bunching (a) Upstream of the MHB, (b) Downstream of the MHB, (c) Upstream of the velocity equalizer, (d) Downstream of the velocity equalizer, (e) At the entrance of the RFQ and (f) At the entrance of the RFQ